

# A study of carbobenzoxy-D-phenylalanine-L-phenylalanine-glycine, an inhibitor of membrane fusion, in phospholipid bilayers with multinuclear magnetic resonance

Andrew R. Dentino<sup>a,1</sup>, Philip W. Westerman<sup>b</sup>, Philip L. Yeagle<sup>a,\*</sup>

<sup>a</sup> Department of Biochemistry, School of Medicine and Biomedical Sciences, State University of New York at Buffalo, 140 Farber Hall, Buffalo, NY 14214, USA

<sup>b</sup> Department of Biochemistry, Northeastern Ohio Universities College of Medicine, Rootstown, OH 44272, USA

Received 4 July 1994; revised 12 October 1994; accepted 18 November 1994

## Abstract

The anti-viral and membrane fusion inhibitor, carbobenzoxy-D-phenylalanine-L-phenylalanine-glycine (ZfFG), was studied in phospholipid bilayers, where earlier studies had indicated this peptide functioned. Multinuclear magnetic resonance (NMR) studies were performed with isotopically labeled peptide. A peptide labeled in the glycine carboxyl with <sup>13</sup>C was synthesized, and the isotropic <sup>13</sup>C-NMR chemical shift of that carbon was measured as a function of pH. A pK<sub>a</sub> of 3.6 for the carboxyl was determined from the peptide bound to a phosphatidylcholine bilayer. ZfFG inhibits the formation by sonication of highly curved, small unilamellar vesicles. Experiments as a function of pH revealed that this ability of ZfFG was governed by a pK<sub>a</sub> of 3.7. Therefore the protonation state of the carboxyl of ZfFG appeared to regulate the effectiveness of this anti-viral peptide at destabilizing highly curved phospholipid assemblies. Such destabilization had previously been discovered to be related to the mechanism of the anti-fusion and anti-viral activity of this peptide. The location of the carboxyl of ZfFG in the membrane was probed with paramagnetic relaxation enhancement of the <sup>13</sup>C spin lattice relaxation of the carboxyl carbon in the glycine of ZfFG (enriched in <sup>13</sup>C). Results suggested that this carboxyl is at or above the surface of the phospholipid bilayer. The dynamics of the molecule in the membrane were examined with <sup>2</sup>H-NMR studies of ZfFG, deuterated in the  $\alpha$ -carbon protons of the glycine. When ZfFG was bound to membranes of phosphatidylcholine, a sharp <sup>2</sup>H-NMR spectral component was observed, consistent with a disordering of the glycine methylene segment of the peptide. When ZfFG was bound to *N*-methyl dioleoylphosphatidylethanolamine (*N*-methyl DOPE) bilayers at temperatures below 30°C, a large quadrupole splitting was observed. These results suggest that ZfFG likely inhibits membrane fusion from the surface of the lipid bilayer, but not by forming a tight, stoichiometric complex with the phospholipids.

**Keywords:** Multinuclear magnetic resonance; Membrane fusion; Anti-viral peptide; NMR

## 1. Introduction

The anti-viral peptide, carbobenzoxy-D-phenylalanine-L-phenylalanine-glycine (ZfFG) was observed to inhibit viral infection of the paramyxoviruses including Sendai, measles, CDV, and SV5 [1]. Recent studies revealed that this peptide inhibited viral infection, both Sendai and measles, by inhibiting membrane fusion, a required step in

viral entry [2–4]. Membrane fusion was inhibited by ZfFG in Sendai fusion with erythrocyte ghosts, Sendai fusion with large unilamellar vesicles (LUV) of *N*-methyl dioleoylphosphatidylethanolamine (*N*-methyl DOPE), and fusion of LUV of *N*-methyl DOPE, and fusion of measles with cells. The inhibition of fusion was specific for the primary structure of the anti-viral peptide. The same structural specificity observed in inhibition of viral infection was also observed in the inhibition of membrane fusion by these anti-viral peptides. More recently, the inhibition of membrane fusion by ZfFG was correlated with an inhibition of the formation of highly curved phospholipid surfaces [5], including those found in hexagonal II phases [6].

\* Corresponding author. Fax: +1 (716) 8292725.

<sup>1</sup> Present address: School of Dentistry, Marquette University, 604 North Sixteenth Street, Milwaukee, WI 53233, USA.

Such observations suggested that the inhibition of membrane fusion was due to the inhibition of the formation of intermediates on the fusion pathway that incorporated highly curved phospholipid surfaces in their structure. In particular, ZfFG altered the packing of lipids in the membrane, favoring relatively flat bilayer structures and destabilizing highly curved phospholipid assemblies [5].

As part of a process designed to better understand the molecular mechanism by which the ZfFG and related peptides inhibited membrane fusion, we studied the behavior of the peptide itself in phospholipid bilayers, using isotopically labeled peptide and multinuclear magnetic resonance (NMR). Using  $^{13}\text{C}$ -enriched peptide, the  $\text{pK}_a$  was determined for the terminal carboxyl of the peptide, in the membrane. ZfFG inhibits the formation of highly curved, small unilamellar vesicles by sonication. Experiments as a function of pH revealed that this ability of ZfFG was governed by a  $\text{pK}_a$  that was the same as that for the ionization reaction of the terminal carboxyl. Some information was obtained about the location of the peptide by measuring the paramagnetic enhancement of spin lattice relaxation from a spin label in the membrane, using the same  $^{13}\text{C}$ -enriched peptide and the observable  $^{13}\text{C}$  resonances from the lipid in the bilayer. Results suggested that this carboxyl was near the surface of the phospholipid bilayer. The dynamics of the peptide were explored with  $^2\text{H}$ -NMR of a specifically deuterated peptide in phospholipid bilayers. The peptide was disordered under conditions where fusion inhibition had previously been observed.

## 2. Materials and methods

Egg phosphatidylcholine (PC), dipalmitoylphosphatidylcholine (DPPC) and *N*-methyl dioleoylphosphatidylethanolamine (*N*-methyl DOPE) were obtained from Avanti Polar Lipids (Birmingham, AL). Carbobenzoxy-D-Phe-L-PheGly (Z-D-Phe-L-PheGly) and carbobenzoxy-Gly-L-Phe were purchased from Sigma (St. Louis, MO). All chemicals and solvents were of the highest purity available and used without further purification. Carbobenzoxy (Z)-D-phenylalanine and L-phenylalanine-OMe hydrochloride, 1-hydroxybenzotriazole (HOBt), 1-ethyl-3-(3-dimethylaminopropyl) carbodiimide (EDC), isobutyl chloroformate, *N*-methylmorpholine, triethylamine and other reagents for peptide synthesis were from Sigma (St. Louis, MO). Thionyl chloride was from Aldrich (Milwaukee, WI). Isotopically labelled residues,  $^2\text{H}$ -Gly ( $\text{d}_5$ , 98%) and  $^{13}\text{C}$ -Gly ( $\text{C}_1$ , 99%), were from Cambridge Isotopes (Woburn, MA).

### 2.1. Phosphate assay

Phosphate was determined by published procedures (Bartlett [18]).

### 2.2. Peptide synthesis and purification

Isotopically labelled residues,  $^2\text{H}$ -Gly (2,2- $\text{d}_2$ , 98%) and  $^{13}\text{C}$ -Gly ( $\text{C}_1$ , 99%) were esterified [7]. The peptide Z-D-Phe-L-Phe-OMe was synthesized using standard carbodiimide/1-hydroxybenzotriazole mediated coupling [8]. Base catalyzed hydrolysis of alkyl esters was employed for carboxyl deprotection and the addition of a labelled Gly-OMe residue was accomplished using an isobutylcarbonic acid mixed anhydride coupling procedure [9]. The peptides were purified and analyzed on an Altex semiprep reverse-phase  $\text{C}_{18}$  column ( $10 \times 250$  mm) coupled to a guard column ( $10 \times 50$  mm) employing an acetonitrile/water (each with 0.1% TFA) linear gradient elution (flow rate:  $1.5 \text{ ml min}^{-1}$ ) mode with detection at 230 nm. The purity of the labelled peptides was further confirmed by thin-layer chromatography using three different solvent systems ( $\text{CHCl}_3/\text{MeOH}$  (95:5), *n*-BuOH/HOAc/ $\text{H}_2\text{O}$  (4:1:1) and  $\text{CHCl}_3/\text{EtOH}$  (9:1)) with iodine stain for detection. Commercially available ZfFG (Sigma) was run in parallel with the  $^{13}\text{C}$ - and  $^2\text{H}$ -labelled peptides. The  $^1\text{H}$ - and  $^{13}\text{C}$ -NMR spectra of the peptides were consistent with their primary structure.

### 2.3. Vesicle preparation

Large unilamellar vesicles (LUV) were prepared according to methods described previously [10] with further details described by Ellens et al. [11]. The phospholipid was hydrated for 3 h on ice, under  $\text{N}_2$  in the indicated buffer. The lipid suspension was next subjected to 5 freeze-thaw cycles followed by 10 extrusions through a polycarbonate membrane with  $0.1 \mu\text{m}$  pores (Nuclepore, Pleasanton, CA). Vesicles were stored on ice, under  $\text{N}_2$  and were used within 1 day. Vesicles were characterized by negative stain transmission electron microscopy and by gel chromatography as a function of the number of extrusions. After 10 extrusions, no further improvement in homogeneity of vesicle size was seen. Also, no evidence of multilamellar vesicles was observed. According to measurements of the electron micrographs, the LUV ranged in size from 200 nm to 900 nm, with most LUV near 400 nm. Encapsulation volume of the LUV was found to be approximately  $12 \mu\text{l}$  per  $\mu\text{mole}$  of phospholipid.

### 2.4. Sonication

Sonication was performed with a Branson W350 probe sonicator with an ice bath at  $0^\circ\text{C}$ , with the probe tuned for the most efficient sonication (output control at 2, continuous output). First, multilamellar liposomes containing the peptide in the phospholipid bilayer were prepared in the following manner. Egg phosphatidylcholine and Z-D-Phe-L-PheGly were co-solubilized in chloroform/methanol (2:1) at room temperature in the indicated molar ratios.

The solvent was removed by evaporation under a stream of nitrogen gas followed by evaporation under high vacuum overnight. The material was then hydrated in H<sub>2</sub>O with 50 mM NaCl and 1 mM Hepes, 1 mM acetic acid, sealed under nitrogen gas and vortexed vigorously. The pH was adjusted to the desired value. The membranes were then treated with five minute sonications followed by a one minute rest period. The light scattering of the sample was determined as effective absorbance at 400 nm at each of the five minute timepoints. This process was repeated 3-times, by which the static light scattering of a sample of egg PC without ZfFG had been reduced to a minimum value. The percentage of effective sonication was determined by comparison of the sample containing ZfFG with the pure egg PC sample:  $((\text{initial light scattering of PC} + \text{ZfFG sample} - \text{final light scattering of PC} + \text{ZfFG sample}) / (\text{initial light scattering of pure PC sample} - \text{final light scattering of pure PC sample})) \times 100$ .

### 2.5. NMR measurements

<sup>2</sup>H-NMR spectra were recorded at 30.87 MHz on a 'home-built' spectrometer. The  $\pi/2$  pulse width was 3–4.5  $\mu$ s, which is adequate power for the <sup>2</sup>H-NMR spectra in the system investigated. A modified quadrupole echo sequence was used for data acquisition [12]. Typically the value of  $\tau$  in the quadrupole echo sequence was 40  $\mu$ s, and the pulse sequence was normally repeated twice per second. Spectra were recorded 'on-resonance' using quadrature detection. Sample temperature was controlled by a computer-controlled liquid (ethylene glycol/H<sub>2</sub>O) flow system, to an accuracy of less than 0.05°C in a single coil probe head with a temperature gradient of less than 0.1°C across the sample.

<sup>1</sup>H-NMR spectra were obtained at 400 MHz in a 5 mm probe using normal single pulse acquisitions on a Bruker

multinuclear Fourier transform-NMR spectrometer. <sup>13</sup>C-NMR (67 MHz) data were obtained on a Jeol FX270 multinuclear Fourier transform-NMR spectrometer in 10 mm tubes, using a 50 kHz window. 2048 data points were collected in the time domain. <sup>13</sup>C-NMR spectra were obtained with a Hahn echo ( $\pi/2 = 7 \mu$ s) and a 1 s repeat time. For measurements of spin lattice relaxation time, the inversion-recovery sequence was used ( $\pi - \tau - \pi/2$ ). Temperature was maintained by a computer-controlled air-flow system.

### 2.6. Data analysis

The titration data were analyzed using a least squares fit of the appropriate sigmoidal equation, using SigmaPlot™.

## 3. Results

### 3.1. *pK<sub>a</sub>* of carboxyl of ZfFG

The carboxyl carbon of ZfFG was enriched to 99% in <sup>13</sup>C as described in Materials and methods, using <sup>13</sup>C-labeled glycine. This labeled peptide was then incorporated into LUV of egg PC by co-solubilizing the peptide with the phospholipid in organic solvent prior to making the LUV. <sup>13</sup>C-NMR spectra were then obtained of this preparation as a function of pH of the medium. The <sup>13</sup>C-NMR spectrum of the LUV plus the <sup>13</sup>C-labeled peptide showed a prominent resonance in the region of 173–176 ppm (depending upon pH) in addition to the phospholipid resonances, due to the carboxyl carbon of the ZfFG (resonance 1 in Fig. 1). The carbonyl resonances of the phospholipids underlay the resonance from the peptide and were not observable relative to the strong signal from the <sup>13</sup>C-enriched peptide carboxyl. Only the phospholipid carbonyl resonances were observed in samples without the labeled ZfFG. The isotropic <sup>13</sup>C chemical shift of the peptide carboxyl resonance was measured as a function of pH. The results are presented in Fig. 2, which represent data from two independent experiments. A least squares fit of the data (see solid line in figure) indicates a *pK<sub>a</sub>* of the carboxyl of ZfFG of 3.6.

### 3.2. Effect of pH on the ability of ZfFG to inhibit the formation of SUV

Previously it was shown that, in the sonication of egg phosphatidylcholine to form small unilamellar vesicles (SUV), the presence of ZfFG was inhibitory [3,5]. Substantial inhibition was previously observed at 25 mol% ZfFG (with respect to the phospholipid component). Therefore in these experiments, 25 mol% ZfFG was added to egg phosphatidylcholine before hydration. The pH was adjusted to the desired value for the experiments. As can be seen in Fig. 3, at pH 3 and 25 mol% ZfFG, a complete

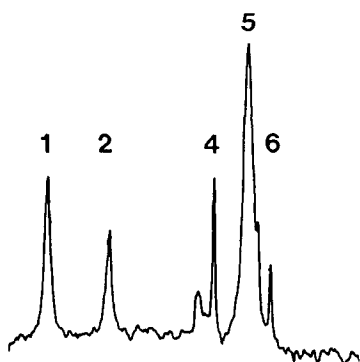


Fig. 1. 67 MHz <sup>13</sup>C-NMR spectra of egg PC LUV (50 mg) containing ZfFG labeled with <sup>13</sup>C in the glycine carboxyl carbon (10 mg). Measurements were made in 1 mM Hepes, 50 mM NaCl, 1 mM EDTA. 6500 transients were accumulated for each spectrum. Peak 1 arises from the <sup>13</sup>C-labeled carboxyl of the ZfFG, peak 2 arises from the vinyl carbons of the phospholipid, peak 4 from the *N*-methyls of the PC headgroup, peak 5 from the methylenes of the hydrocarbon chains from the PC, and peak 6 from the terminal methyl of the hydrocarbon chains.

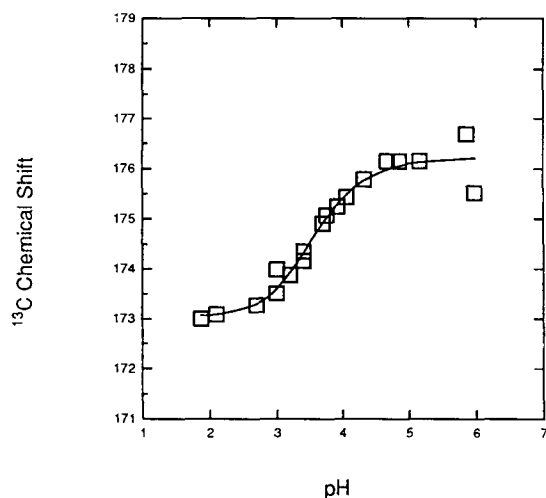


Fig. 2. Chemical shift of the  $^{13}\text{C}$ -NMR resonance from the glycine carboxyl carbon ( $^{13}\text{C}$ -labeled) of ZfFG in egg PC LUV as a function of pH. The solid line is a fitted curve with a  $\text{p}K_a$  of 3.6. Spectra were accumulated as in Fig. 1 and as described in Materials and methods.

inhibition of formation of SUV was observed (no detectable reduction in light scattering upon sonication as described in Materials and methods). This effect is reduced as the pH is increased, until at pH 5.5 and greater, a maximum of about 25% inhibition of the sonication process was recorded. The curve in Fig. 3 can be fit with a  $\text{p}K_a$  of 3.7. It should be noted that these data indicate an inhibition of the process of formation of SUV by sonication at all pH values; however, the maximum effect was produced by ZfFG when the carboxyl was protonated. Thus at low pH, less peptide is required to inhibit formation of SUV than at high pH.

### 3.3. Relaxation enhancement of $^{13}\text{C}$ $T_1$ of phospholipid and peptide resonances by the 16-doxyl spin label

$T_1$  measurements were made on  $^{13}\text{C}$  resonances of egg PC and the  $^{13}\text{C}$  resonance of ZfFG labeled with  $^{13}\text{C}$  in the glycine carboxyl carbon, as a function of added spin label (the 16-doxyl fatty acid spin label). Measurements were made on LUV of egg PC containing labeled peptide at 20 mole percent (peptide with respect to the phospholipids). The spin label was added prior to formation of the LUV. Higher resolution experiments with SUV were not possible due to the inhibition of the formation of SUV by ZfFG. Therefore, only clearly resolvable single carbon resonances were measured, including the *N*-methyl carbon resonance, the vinyl carbon resonances, and the terminal methyl carbon resonance of the phosphatidylcholine. The  $T_1$  of these resonances in the absence of spin label and peptide were the same as reported previously [13]. The enhancement of relaxation was then calculated according to the following equation:

$$\frac{1}{T_{1e}} = \frac{1}{T_{1s}} - \frac{1}{T_{1n}}$$

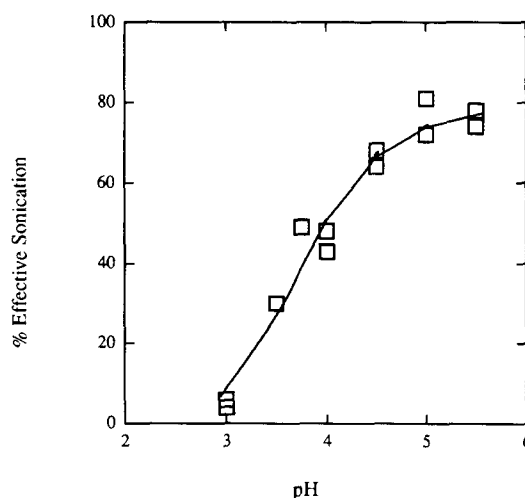


Fig. 3. Effectiveness of ZfFG at inhibiting the formation of SUV by sonication as a function of pH, following the procedures described in the text. The solid line is a fitted curve with a  $\text{p}K_a$  of 3.7.

where  $T_{1e}$  is the enhancement of the relaxation time,  $T_{1s}$  is the relaxation in the presence of spin label and  $T_{1n}$  is the relaxation in the absence of spin label. Fig. 4 shows the relaxation enhancement of the resolvable individual carbons in the  $^{13}\text{C}$ -NMR spectrum as a function of spin label concentration in the bilayer. (Since these measurements were made on LUV, the resonances were, in general, broad. Only the  $T_1$  of those resonances of carbons that occurred with a chemical shift well removed from the other carbons were therefore measured.) At 3 mol% spin label, the effects were small and ambiguous. However, at 7 mol% spin label, the relaxation enhancement of each of the carbons was clearly distinguishable from each of the other carbons. The most strongly perturbed resonance of the phospholipid was the vinyl resonance. At the highest spin label concentration used, the least perturbed  $T_1$  was that of the peptide carboxyl carbon.

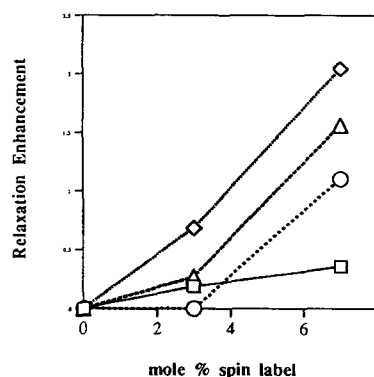


Fig. 4. Relaxation enhancement,  $1/T_{1e}$ , for three carbons from PC and from the carboxyl carbon ( $^{13}\text{C}$ -enriched) of the glycine of ZfFG, in LUV of egg PC, as a function of the mole percent added fatty acid spin label ( $\text{C}_{16}$ ). Measurements were made in the same buffer as in Fig. 1. (□) ZfFG carboxyl carbon (glycine); (Δ) terminal methyl carbons of the hydrocarbon chains of PC; (◇) vinyl carbons of PC; (○) *N*-methyl carbons of PC.

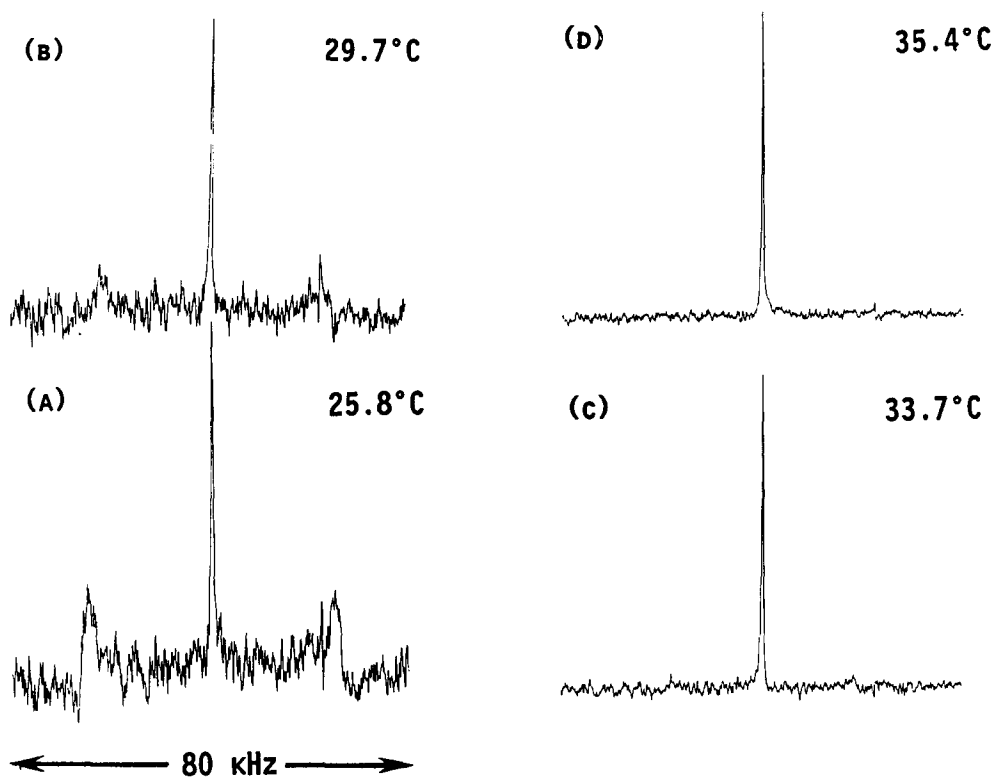


Fig. 5. 30.87 MHz  $^2\text{H}$ -NMR spectra of a sample containing  $^2\text{H}$ -labeled ZfFG (10 mg) and *N*-methyl DOPE (37.5 mg) (peptide/phospholipid molar ratio = 2.5:1) dispersed in 250  $\mu\text{l}$  of  $^2\text{H}$ -depleted water with 1 mM Hepes, 50 mM NaCl, at pH 3: (A) 25.8°C, (B) 29.7°C, (C) 33.7°C and (D) 35.4°C. Spectra were obtained from 40 000 to 60 000 transients. The accumulated free-induction decay was multiplied by the same line-broadening function in each case.

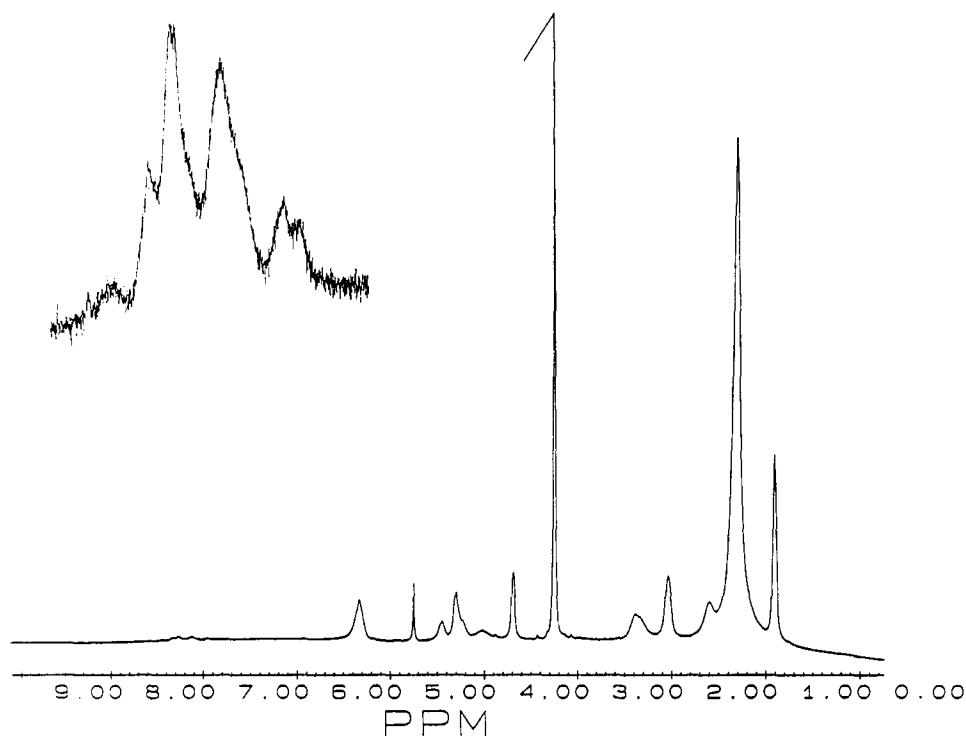


Fig. 6. 400 MHz  $^1\text{H}$ -NMR spectra of ZfFG added to preformed SUV of egg PC in 1 mM Hepes,  $^2\text{H}_2\text{O}$ , and a small amount of  $\text{CD}_3\text{OH}$  for addition of the peptide, at pH 7. The  $^1\text{H}$  resonances from the phenyl rings of the ZfFG are clearly visible in the vicinity of 8 ppm. Inset: expansion of the aromatic region showing the resonances from the aromatic protons of the ZfFG.

### 3.4. Behavior of ZfFG in phospholipid bilayers from $^2\text{H}$ -NMR spectra of $^2\text{H}$ -labeled peptide

ZfFG was labeled with  $^2\text{H}$  by synthesis with [2,2- $^2\text{H}_2$ ]glycine. This peptide was incorporated into phospholipid bilayers composed of egg PC and in bilayers composed of *N*-methyl DOPE by co-solubilization in  $\text{CHCl}_3/\text{CH}_3\text{OH}$  before hydration to form MLV. The former was used because it presented a stable lamellar phase and the latter lipid was used because of the ability of ZfFG to inhibit fusion of *N*-methyl DOPE LUV at temperatures above  $35^\circ\text{C}$ .  $^2\text{H}$ -NMR measurements were made in  $^2\text{H}$ -depleted media. The peptide content was (relative to the phospholipid content) modestly higher than the level of ZfFG required to maximally inhibit membrane fusion [2,3]. In egg PC bilayers, a sharp spectral component was observed from the deuterated ZfFG at all temperatures measured (data not shown). In *N*-methyl DOPE bilayers, only a sharp spectral component was observed at temperatures of  $35^\circ\text{C}$  and above. At slightly lower temperatures ( $33.7^\circ\text{C}$ ) a powder pattern with  $90^\circ$  edge singularities separated by 36 kHz was evident (Fig. 5C). At  $29.7^\circ\text{C}$ , a powder pattern with splitting  $50 \pm 1$  kHz was observed (Fig. 5B). The intensity of this broad spectral component relative to the sharp spectral component increased with cooling until a temperature of  $25^\circ\text{C}$  was reached (Fig. 5A). The sharp spectral component did not disappear with further cooling but represented an insignificant proportion of the total signal. The peak probably arose from natural abundance deuterium in the buffer solute, Hepes, or from inadvertent exchange with atmospheric water during the sample manipulation. The spectral changes with temperature described above were completely reversible. The results were reproduced with two independent syntheses of the deuterated peptide. The unhydrated powder of the pure deuterated peptide was also recorded and exhibited a quadrupole splitting of  $50 \pm 1$  kHz (data not shown).

### 3.5. Behavior of ZfFG in phospholipid bilayers from $^1\text{H}$ -NMR spectra

High resolution 400 MHz  $^1\text{H}$ -NMR spectra were obtained of ZfFG added to preformed SUV of egg PC. Under conditions of near neutral pH and limited amounts of added ZfFG ( $\leq 10$  mol% with respect to the PC), such samples were observed to be metastable for several hours, sufficient to obtain the NMR spectra. (Over longer time periods, the SUV degraded and the suspension became turbid and unsuitable for high resolution-NMR studies. Lower pH and higher concentrations of ZfFG led to unacceptably high rates of degradation of the integrity of the SUV.) Fig. 6 shows a typical  $^1\text{H}$ -NMR spectrum of such a preparation. In addition to the resonances of the phospholipid, resonances arising from the phenyl rings of the ZfFG could be observed downfield at about 8 ppm (the substantial broadening consistent with the conclusion reached

previously that the peptide is bound to the membrane and is not free in solution [3]).

## 4. Discussion

The  $\text{pK}_a$  of the carboxyl of the ZfFG was found to be 3.6. The effectiveness of the ZfFG at inhibiting SUV formation was consistent with the ionization of the peptide carboxyl. The protonated form was the most effective under these conditions, although both the protonated and the unprotonated form were effective at interfering with the process of SUV formation. Previous work had revealed that ZfFG inhibited the formation of highly curved phospholipid assemblies. This work has indicated that the protonated form of the anti-viral peptide was the most potent inhibitor of the formation of curved surfaces. Perhaps the protonated form penetrated deeper into the membrane than the charged form of the peptide, thereby more strongly influencing the behavior of the phospholipids.

The data on enhancement of  $^{13}\text{C}$  spin lattice relaxation indicates that the peptide carboxyl was well-removed from the center of the bilayer. Under the most simple of conditions, the paramagnetic enhancement of spin lattice relaxation is inversely proportional to the sixth power of the distance between the  $^{13}\text{C}$  nucleus and the unpaired electron of the spin label. In this specific case, the relationship is quantitatively a more complicated one, involving the lateral diffusion of the spin label and the peptide. However, this can be considerably simplified if one is interested only in the relative distances between known positions on the lipids and the spin label, compared to the distance between the  $^{13}\text{C}$ -labeled carboxyl and the spin label.

$$\frac{1}{T_{1e}} \propto g(\tau) \frac{1}{r^6}$$

where  $g(\tau)$  is the correlation function describing the time dependence of the dipolar interactions between the unpaired electron and the relevant  $^{13}\text{C}$  nucleus. This function is, in principle, complex due to the anisotropy of the relevant molecular dynamics and the lateral diffusion in the system [14]. However, if to a first approximation  $g(\tau)$  is the same for each of the nuclear spin–electron spin interactions involved (for example the influence of lateral diffusion would be expected to be similar for each of the interactions), then a comparison of  $1/T_{1e}$  for different carbons will provide a measure of the ratio of the electron–nuclear separation,  $r$  (larger  $1/T_{1e}$  corresponds to smaller  $r$ ).

The applicability of this relationship can be tested on the data from the  $^{13}\text{C}$  resonances from particular carbons of the phospholipid. With a spin label located in the interior of the bilayer, one would expect a stronger enhancement,  $1/T_{1e}$ , for the terminal methyl and the vinyl carbons than for the *N*-methyl carbons in the headgroup. As observed in Fig. 4, this expectation is fulfilled. Then

consideration of  $1/T_{1e}$  for the peptide carbonyl carbon shows that it is the least affected of the individual carbons measured. The  $1/T_{1e}$  for the carbonyl carbon is nearly an order of magnitude less than  $1/T_{1e}$  for the vinyl carbons, which are the closest to the position of the spin label in the bilayer.  $1/T_{1e}$  for the peptide carbonyl carbon is less than  $1/T_{1e}$  for the phosphatidylcholine *N*-methyl carbons. Quantitative comparisons need to be made carefully here, since the dynamics of the *N*-methyl carbons are different than the dynamics of the hydrocarbon chain carbons. However, it is still reasonable to conclude that the peptide terminal carbonyl is most likely located on the surface of the membrane and not in the interior of the membrane. Such a conclusion is also consistent with the  $pK_a$  of the carboxyl which is not indicative of a carbonyl buried in a medium of low dielectric constant. A surface location for the terminal carbonyl is consistent with its strongly polar character.

The  $^2\text{H}$ -NMR data on the  $^2\text{H}$ -labeled ZfFG showed no significant ordering of the peptide glycine when ZfFG was bound to bilayers of *N*-methyl DOPE at temperatures at which the peptide had been observed previously to inhibit membrane fusion of *N*-methyl DOPE LUV. In particular, at temperatures of 35°C and above, only a sharp spectral component was observed in the  $^2\text{H}$ -NMR of bilayers of *N*-methyl DOPE, characteristic of a disordered state of the peptide. Previous studies [2] showed that ZfFG inhibited membrane fusion of *N*-methyl DOPE LUV at temperatures of 35°C and above and fusion of Sendai virus with *N*-methyl DOPE LUV (fusion rates in these systems below 35°C were too low to detect significant inhibition).

At all temperatures, the  $^2\text{H}$ -NMR data showed a sharp spectral component from  $^2\text{H}$ -labeled ZfFG in PC bilayers. ZfFG showed inhibition of Sendai fusion with erythrocyte ghosts at all temperatures between 25°C and 40°C [3], in which ZfFG was introduced into the outer leaflet of the erythrocyte, composed mainly of PC and sphingomyelin.

Therefore it was unlikely that the peptide was oriented in the membrane analogously to the lipids or to cholesterol (director for axial diffusion perpendicular to the membrane surface) as part of the mechanism of inhibition of membrane fusion. Such a location would be likely to produce measurable quadrupole splittings from the deuterated positions due to additional restriction on modes of motion of the peptide, imposed by the ordering of the membrane structure. Rather the observed dynamic behavior was consistent with a location of the peptide on the surface of the membrane.

There is an alternative explanation for the  $^2\text{H}$ -NMR data that cannot be ruled out on the basis of these studies alone: a time-averaged orientation of the C–D bond segments at the ‘magic angle’ with respect to the director for axial diffusion leading to the observed sharp spectral component. However, high resolution  $^1\text{H}$ -NMR measurements of ZfFG added to preformed SUV of egg PC showed observable, though broadened, resonances due to the phenyl

rings of the peptide (Fig. 6), supporting the suggestion above that the peptide was disordered in the membrane surface. For comparison, no  $^1\text{H}$ -NMR resonances were observed from the motionally ordered portions of cholesterol in SUV of PC [15]. Furthermore, it should be noted that the available evidence suggests that the peptide is largely bound to the membrane (and not in solution, where an isotropic resonance would result). A complex of the peptide with phospholipid, forming a mixed micelle and producing an isotropic resonance, can be ruled out on the basis of the  $^{31}\text{P}$ -NMR data which does not show an isotropic component for the phospholipids [3].

At temperatures below 35°C, a highly ordered component was observed from the ZfFG in bilayers of *N*-methyl DOPE. These  $^2\text{H}$ -NMR data indicated that the ZfFG had access to at least two ‘sites’ in the sample at low temperature and that there was an equilibrium of ZfFG distribution between these two sites. The similarity of the quadrupole splittings from [2,2  $d_2$  gly]ZfFG in *N*-methyl DOPE at 25°C and the splitting from the pure [2,2  $d_2$  gly]ZfFG in a powder suggested that the peptide was excluded from the *N*-methyl DOPE bilayer at low temperature. Perhaps this could have been the result of increased hydrogen bonding between the quaternary amines and the phosphate of a neighboring phospholipid. Such hydrogen bonding has been shown to be important to the behavior of bilayers of derivatized phosphatidylethanolamine [16]. It was not a result of an  $L_\alpha$ – $H_{II}$  phase transition, the phase boundary for which has been reported at a significantly higher temperature for the pure lipid [17]. The  $L_\alpha$ – $H_{II}$  transition temperature for phosphatidylethanolamines is increased by the presence of ZfFG [6].

It can be speculated that ZfFG is likely on the surface of the membrane, perhaps with its hydrophobic phenyl rings extending toward the hydrophobic part of the membrane, and not immobilized, when it is inhibiting membrane fusion and the formation of highly curved phospholipid assemblies. ZfFG is not likely tightly bound to a phospholipid, in a 1:1 or 1:2 complex or similar, but is more likely rapidly exchanging among sites on the membrane surface. Thus, while it takes about 25 mol% to obtain the maximal effect of the peptide on function, nevertheless, that is probably less peptide than would be required if a tight complex with phospholipid was formed.

## Acknowledgements

We thank Dr. J. Alderfer for making the instrument available for the  $^1\text{H}$ -NMR measurements. This work was supported by National Institutes of Health Grant AI26800 and DE05608.

## References

- [1] Richardson, C.D., Scheid, A. and Choppin, P.W. (1980) *Virology* 105, 205–222.

- [2] Kelsey, D.R., Flanagan, T.D., Young, J. and Yeagle, P.L. (1990) *J. Biol. Chem.* 265, 12178–12183.
- [3] Kelsey, D.R., Flanagan, T.D., Young, J. and Yeagle, P.L. (1991) *Virology* 182, 690–702.
- [4] Harrowe, G., Mitsuhashi, M. and Payan, D.G. (1990) *J. Clin. Inv.* 85, 1324–1327.
- [5] Yeagle, P.L., Young, J., Hui, S.W. and Epand, R.M. (1992) *Biochemistry* 31, 3177–3183.
- [6] Epand, R.M. (1986) *Biosci. Rep.* 6, 647–653.
- [7] Brenner, M. and Huber, W. (1953) *Helv. Chim. Acta* 36, 1109–1115.
- [8] Konig, W. and Geiger, R. (1970) *Chem. Ber.* 103, 2034.
- [9] Bodanszky, M. (1984) *Principles of peptide synthesis*, Springer-Verlag, New York, NY.
- [10] Szoka, F., Olson, F., Heath, T., Vail, W., Mayhew, E. and Papahadjopoulos, D. (1980) *Biochim. Biophys. Acta* 601, 559–571.
- [11] Ellens, H., Siegel, D.P., Alford, D., Yeagle, P.L., Boni, L., Lis, L.J., Quinn, P.J. and Bentz, J. (1989) *Biochemistry* 28, 3692–3703.
- [12] Rance, M., Jeffrey, K.R., Tullock, A.P., Butler, K.W. and Smith, I.C.P. (1980) *Biochim. Biophys. Acta* 600, 245–262.
- [13] Yeagle, P.L. and Frye, J. (1987) *Biochim. Biophys. Acta* 899, 137–142.
- [14] Brulet, P. and McConnell, H.M. (1975) *Proc. Natl. Acad. Sci. USA* 72, 1451–1455.
- [15] Kroon, P.A., Kainosho, M. and Chan, S.I. (1975) *Nature (London)* 256, 582–584.
- [16] Brown, P.M., Steers, J., Hui, S.W., Yeagle, P.L. and Silvius, J.R. (1986) *Biochemistry* 25, 4259–4267.
- [17] Gagne, J., Stamatatos, L., Diacovo, T., Hui, S.W., Yeagle, P.L. and Silvius, J. (1985) *Biochemistry* 24, 4400–4408.
- [18] Bartlett, G.R. (1959) *J. Biol. Chem.* 234, 466–473.